universe

MDPI

Article

A Fit to the Available $e^+e^- \to \Lambda_c^+ \bar{\Lambda}_c^-$ Cross Section Data Nearby Production Threshold by Means of a Strong Correction to the Coulomb Enhancement Factor

Antonio Amoroso [1,2], Stefano Bagnasco [1], Rinaldo Baldini Ferroli [3,4], Ilaria Balossino [3,5], Monica Bertani [4], Diego Bettoni [5], Fabrizio Bianchi [1,2], Alberto Bortone [1,2], Alessandro Calcaterra [4], Gianluigi Cibinetto [5], Fabio Cossio [1], Francesca De Mori [1,2], Manuel Dioniso Da Rocha Rolo [1], Marco Destefanis [1,2], Riccardo Farinelli [5], Luciano Fava [1], Giulietto Felici [4], Luciano Gaido [1], Isabella Garzia [5,6], Stefano Gramigna [5,6], Michela Greco [1,2], Lia Lavezzi [1,2], Stefano Lusso [1], Marco Maggiora [1,2], Alessio Mangoni [7], Simonetta Marcello [1,2], Giulio Mezzadri [3,5,*], Sara Morgante [1,2], Elisabetta Pace [4], Simone Pacetti [7,8], Piero Patteri [4], Angelo Rivetti [1], Marco Scodeggio [5,6], Stefano Sosio [1,2] and Stefano Spataro [1,2]

1 INFN—Sezione di Torino, Via P. Giuria 1, 10125 Torino, Italy; amoroso@to.infn.it (A.A.); bagnasco@to.infn.it (S.B.); bianchi@to.infn.it (F.B.); abortone@to.infn.it (A.B.); fcossio@to.infn.it (F.C.); demori@to.infn.it (F.D.M.); darochar@to.infn.it (M.D.D.R.R.); destefanis@to.infn.it (M.D.); fava@to.infn.it (L.F.); gaido@to.infn.it (L.G.); greco@to.infn.it (M.G.); lavezzi@to.infn.it (L.L.); lusso@to.infn.it (S.L.); maggiora@to.infn.it (M.M.); smorgant@to.infn.it (S.M.); marcello@to.infn.it (S.M.); rivetti@to.infn.it (A.R.); sosio@to.infn.it (S.S.); spataro@to.infn.it (S.S.)
2 Dipartimento di Fisica, Università degli Studi di Torino, Via P. Giuria 1, 10125 Torino, Italy
3 Institute of High Energy Physics, Chinese Academy of Sciences, 19B Yuquan Road, Beijing 100049, China; rinaldo.baldini@lnf.infn.it (R.B.F.); balossino@fe.infn.it (I.B.)
4 INFN—Laboratori Nazionali di Frascati, Via E. Fermi 40, 00044 Frascati, Italy; monica.bertani@lnf.infn.it (M.B.); alessandro.calcaterra@lnf.infn.it (A.C.); giulietto.felici@lnf.infn.it (G.F.); elisabetta.pace@lnf.infn.it (E.P.); piero.patteri@lnf.infn.it (P.P.)
5 INFN—Sezione di Ferrara, Via G. Saragat 1, 44122 Ferrara, Italy; bettoni@fe.infn.it (D.B.); cibinett@fe.infn.it (G.C.); rfarinelli@fe.infn.it (R.F.); garzia@fe.infn.it (I.G.); stefano.gramigna@edu.unife.it (S.G.); mscodegg@fe.infn.it (M.S.)
6 Dipartimento di Fisica e Scienze della Terra, Università degli Studi di Ferrara, Via Saragat 1, 44122 Ferrara, Italy
7 INFN—Sezione di Perugia, Via A. Pascoli, 06123 Perugia, Italy; mangoni@pg.infn.it (A.M.); pacetti@pg.infn.it (S.P.)
8 Dipartimento di Fisica e Geologia, Università degli Studi di Perugia, Via A. Pascoli, 06123 Perugia, Italy
* Correspondence: gmezzadr@fe.infn.it

Citation: Amoroso, A.; Bagnasco, S.; Baldini Ferroli, R.; Balossino, I.; Bertani, M.; Bettoni, D.; Bianchi, F.; Bortone, A.; Calcaterra, A.; Cibinetto, G.; et al. A Fit to the Available $e^+e^- \to \Lambda_c^+ \bar{\Lambda}_c^-$ cross Section Data Nearby Production Threshold by Means of a Strong Correction to the Coulomb Enhancement Factor. *Universe* **2021**, *7*, 436. https://doi.org/10.3390/universe7110436

Academic Editor: Lorenzo Lorio

Received: 12 September 2021
Accepted: 10 November 2021
Published: 14 November 2021

Abstract: There are two available sets of data on the $e^+e^- \to \Lambda_c^+ \bar{\Lambda}_c^-$ cross section at energies close to the production threshold, collected by the Belle and by the BESIII Collaborations. The measurement of the former, performed by means of the initial state radiation technique, is compatible with the presence of a resonance, called $\psi(4660)$, observed also in other final states. On the contrary, the latter is measured an almost flat and hence non-resonant cross section in the energy region just above the production threshold, but the data stop before the possible rise in the cross section for the resonant production. We propose an effective model to describe the behavior of the data near this threshold, which is based on a Coulomb-like enhancement factor due to the strong interaction among the final state particles. In the framework of this model, it is possible to describe both datasets.

Keywords: hadron spectroscopy; exotic states; particle physics; charmed hyperon cross section

1. Introduction

The measurement of the baryon-anti-baryon cross section from electron-positron annihilation has attracted great interest in recent years, especially in the region near to the production threshold, partially owing to the efforts of the BESIII Collaboration. Although

there are plenty of results for nucleons [1,2] and hyperons [3–5], studies of the charmed baryon are scarce.

The Λ_c particle is the lightest charmed baryon. Having precise knowledge of its properties is of the utmost importance for the study of the other charmed baryons. Moreover, since it can be described as a combination of udc quarks, and being charged, it has several features similar to the proton. Despite this, the knowledge of the behavior of its cross section is limited, with only two datasets available.

The first measurement was performed by the Belle Collaboration using the $e^+e^- \to \gamma_{ISR}\Lambda_c^+\bar{\Lambda}_c^-$ cross section, where γ_{ISR} is the initial state photon emitted by one of the two initial leptons [6]. In that work, they described the data with a resonance, called $\psi(4660)$, observed by Belle [7] and also by the BaBar Collaboration [8] in other final states. This state is overabundant with respect to the conventional charmonium spectrum [9] and it is part of the exotic family called the XYZ state [10].

The second measurement was performed later by the BESIII Collaboration, which collected four data samples on the $\Lambda_c^+\bar{\Lambda}_c^-$ cross section in the energy region close to the production threshold [11]. These data show a different trend with respect to the previous result [6], seeming as if no resonance will appear. However, the data stop exactly at the energy below which the rise in the cross section may be expected.

The first full treatment of the two different behavior was performed in [12] by means of chiral EFT [13,14]. However, when the authors tried to investigate the interplay between the two datasets, they mentioned that it was impossible to reconcile both trends using the model they proposed.

In this paper, we propose a model to explain the phenomenon of the steep rise in the cross section at the threshold, which is described in terms of a Coulomb-like enhancement effect [15], due to the strong interaction of the final baryons. By considering this effect, we also parametrize the lineshape of the cross section in the case of resonant behavior around the $\psi(4660)$ resonance, to show that it is possible to reconcile simultaneously both the available BESIII [11] and Belle [6] datasets. With respect to the original Belle paper, we have removed the first energy value since, due to the ISR center of mass uncertainty, more than half of its center of mass may lie below the $\Lambda_c^+\bar{\Lambda}_c^-$ production threshold. Since the threshold behavior is our focus, we decided to consider only those data that are definitely above it, instead of correcting for the aforementioned effect.

2. The Coulomb Factor

The Born cross section of electron-positron annihilation into an baryon-antibaryon is

$$\sigma(e^+e^- \to B\bar{B}) = \frac{4\pi\alpha^2}{3W^2} C\beta \left[|G_M(W^2)|^2 + 2\frac{M_B^2}{W^2}|G_E(W^2)|^2 \right], \quad (1)$$

where α is the fine-structure constant, β and M_B are the velocity and the mass of the baryon, W is the e^+e^--center of mass energy, G_E and G_M are the Sachs electric and magnetic form factors and C is the so-called Coulomb factor (CF), which is due to the electromagnetic interaction between the charged baryons as $\beta \to 0$. The CF is given by the modulus squared evaluated at $r = 0$ of the wave function $\psi(r)$, describing the non-relativistic electron scattering, and is obtained by solving the Schrödinger equation with the Coulomb potential $V(r) = e^2/r$. Its expression as a function of the velocity β is [16]:

$$C(\beta) = |\psi(0)|^2 = \frac{\pi\alpha\sqrt{1+\beta^2}/\beta}{1 - e^{-\pi\alpha(1+\beta^2)/\beta}}. \quad (2)$$

This form does also include a relativistic correction, obtained by making the substitution $1/\beta \to \sqrt{1+\beta^2}/\beta$ in the original non-relativistic expression. Close to the threshold,

as $\beta \to 0$, the CF behaves like the only numerator function $\pi\alpha\sqrt{1+\beta^2}/\beta$, that, having a simple pole at $\beta = 0$, is usually called the *enhancement factor*

$$E(\beta) = \frac{\pi\alpha\sqrt{1+\beta^2}}{\beta}\,. \tag{3}$$

The most relevant effect of the electromagnetic interaction occurring between the charged baryons just after their formation and when they are very close and almost overlapping, is that exactly at the threshold energy, $W = 2M_B$, and the probability of being produced is abruptly different from zero. As a consequence, the cross section is discontinuous and it rises quickly from zero up to, according to Equation (1),

$$\sigma(e^+e^- \to B\bar{B})_{\text{thr.}} = \frac{\pi^2\alpha^3}{2M_B^2}|G_{\text{thr.}}|^2\,,$$

where $G_{\text{thr.}}$ represents the common value of the electric and magnetic Sachs form factors at the production threshold, i.e., $G_{\text{thr.}} \equiv G_E(4M_B^2) = G_M(4M_B^2)$.

The second factor of the function $C(\beta)$ given in Equation (2), namely the inverse of the denominator in

$$R(\beta) = \frac{1}{1-e^{-\pi\alpha(1+\beta^2)/\beta}}\,, \tag{4}$$

is usually called the Sommerfeld re-summation factor and describes the multiple-photon exchange between the final charged baryons.

The Strong Coulomb-Like Correction

Because of the hadronic nature of the final baryons, a strong correction should also be considered in addition to the pure electromagnetic one. Following the same procedure exploited to obtain the CF, the effect of the gluon exchange that mediates the strong interaction just after the production of the baryon pair, i.e., at $\beta \to 0$, can be described by the function $C_s(\beta)$, obtained by making the substitution $\alpha \to \alpha + \alpha_s$ in Equation (2). The strong coupling constant α_s depends on the energy, decreasing logarithmically as the energy increases, so that, at high energy, i.e., low distances and $\beta \to 0$, $\alpha_s \ll \alpha$ and $C_s(\beta) \simeq C(\beta)$. On the other hand, as β increases, just few MeV above the baryon production threshold, α_s becomes dominant over the fine-structure constant α, and hence

$$C_s(\beta) \simeq \frac{\pi\alpha_s\sqrt{1+\beta^2}/\beta}{1-e^{-\pi\alpha_s\sqrt{1+\beta^2}/\beta}}\,. \tag{5}$$

The phenomenological need of a strong Coulomb-like correction, in addition to the electromagnetic one, arises from the study of the $p\bar{p}$ cross section at the threshold. Indeed, the process $e^+e^- \to p\bar{p}$ represents the prototype reaction in which such a phenomenon manifests itself, having in the final state the lightest pair of charged baryons and, moreover, stable ones.

As a consequence, this cross section is well studied and there are several published measurements [17–21]. Its line-shape exhibits a steep rise just above the threshold to a value that is very close to the prediction of a point-like production [22,23] and then continues with a flat behavior up to 2 GeV. The recent measurement of the CMD3 [19] Collaboration shows that the cross section rises from zero to 0.8 nb in just one MeV. This is a clear manifestation of the threshold discontinuity of the cross section, i.e., a step behavior, that cannot be described by the previous models based on final-state interaction [24–30].

On the contrary, the strong Coulomb-like correction provides a quite reasonable and plausible description of this phenomenon. In particular, following the line of thought developed in the previous sections, the cross section can be parameterized as

$$\sigma(e^+e^- \to p\bar{p}) = \frac{1}{W^2} \frac{2\pi^2\alpha^3\sqrt{1+\beta^2}}{1-e^{-\pi\alpha_s(W)\sqrt{1+\beta^2}/\beta}} |FF|^2 \quad (6)$$

where W is the e^+e^--center of mass energy, M_p is the proton mass. The last factor FF represents the modulus squared of the effective form factor, which depends on two free parameters, i.e., the energy scale Λ_0 and the power N, and can be expressed as

$$|FF|^2 = \frac{1}{1+\left[(W-2M_p)/\Lambda_0\right]^N}$$

Notice that it is normalized to the unity at the production threshold $W = 2M_p$ [22,23].

Figure 1 shows the data and the fit with $\Lambda_0 = (325 \pm 3)$ MeV and $N = (4.9 \pm 0.2)$. This value has to be compared with the theoretical expectation $N^{\text{theo}} = 8$. For the QCD running coupling constant, we used the time-like expression

$$\alpha_s(W) = \frac{4\pi}{\beta_0\sqrt{\ln^2(W^2/\Lambda^2_{\text{QCD}}) + \pi^2}},$$

with $\Lambda_{\text{QCD}} = 350$ MeV and $\beta_0 = 11 - 2n_f/3$; in particular, dealing with energies well below the b quark mass, we used $n_f = 4$, i.e., we assumed that only the three lightest quarks u, d, and s are involved in the observed phenomena, and hence $\beta_0 = 8$.

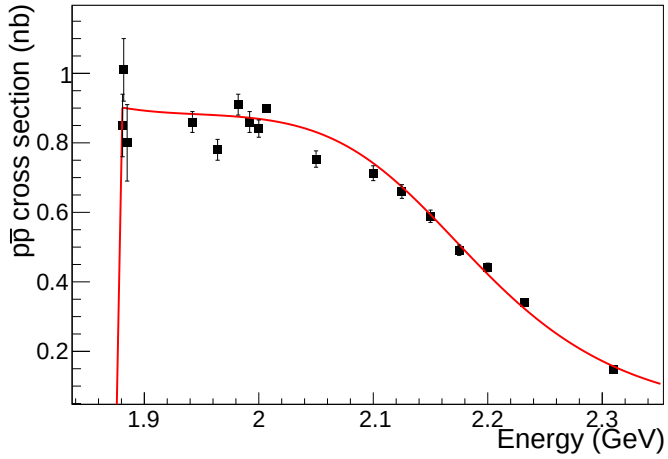

Figure 1. Fit to the most recent BESIII and CMD3 data with the strong corrected Coulomb enhancement factor (CEF). The red line shows the cross section values as fitted from Equation (6), whereas the black dots with error bars indicate the experimental measured values.

3. The Fit to $e^+e^- \to \Lambda_c^+\bar{\Lambda}_c^-$ Cross Section

It is possible to use the same formalism to describe the $e^+e^- \to \Lambda_c^+\bar{\Lambda}_c^-$ cross section. First, we use Equation (6) to describe the non-resonant part of the cross section, that shows a sharp step just above threshold and then a flat behavior. Then, we will add the resonant component to show that both the Belle and BESIII data can be fitted together.

3.1. The Non-Resonant Component

The normalization factor $(2M_{\Lambda_c})^2\sigma^{\Lambda_c}_{\text{thr.}}$, being M_{Λ_c} the Λ_c^+ mass and $\sigma^{\Lambda_c}_{\text{thr.}}$ the value of the cross section at the threshold, was included in Equation (6). As a consequence, the fit function is

$$\sigma(e^+e^- \to \Lambda_c^+\bar{\Lambda}_c^-) = \frac{(2M_{\Lambda_c})^2\sigma^{\Lambda_c}_{\text{thr.}}}{W^2} \frac{2\pi^2\alpha^3\sqrt{1+\beta^2}}{1-e^{-\pi\alpha_s(W)\sqrt{1+\beta^2}/\beta}} \frac{1}{1+\left[(W-2M_{\Lambda_c})/\Lambda_0\right]^N}, \quad (7)$$

where $\sigma_{\text{thr.}}^{\Lambda_c}$, the energy scale Λ_0 and the power N are free parameters to be fitted.

The result of the fit to all the points is shown in Figure 2. The best values of the parameters are $\sigma_{\text{thr.}}^{\Lambda_c} = (239 \pm 10)$ pb, $\Lambda_0 = (163 \pm 19)$ MeV and $N = (7 \pm 4)$. Only the N value will be kept fixed in the following fitting of the resonant line-shape, where all the errors are symmetrical and can be interpreted as 1σ deviations. The fit quality is reasonable, since the reduced $\chi^2 = 2$. This is mainly due to the large error bars of the Belle data. In Table 1 a list of the predicted cross sections in the energy interval between 4.58 and 4.76 GeV is shown in order to make a comparison with the resonant hypothesis.

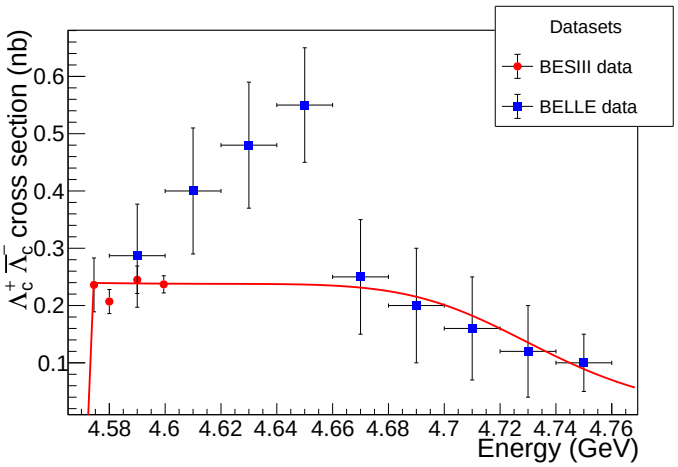

Figure 2. Fit to the available BESIII and Belle data close to the $\Lambda_c^+\bar{\Lambda}_c^-$ threshold, assuming the cross section has only non-resonant behavior. The red dots with error bars are the BESIII experimental data [11], the blue squares are the BELLE data [6], and the red line is the fit result with the formula on Equation (6) modified as described in the text. The first Belle data in Ref. [6] are not presented in the plot, as discussed in the introduction.

Table 1. Summary table of the predicted cross sections in the case of only the non-resonant cross section (σ^{NR}) and resonant one (σ^{R}).

Mass/GeV/c^2	σ^{NR}**/nb**	σ^{R}**/nb**
4.58	0.239	0.221
4.61	0.238	0.299
4.64	0.237	0.587
4.67	0.231	0.282
4.7	0.201	0.190
4.73	0.135	0.133
4.76	0.07	0.071

3.2. Adding the Resonant Component

Finally, we add to the expression for the non-resonant cross section of Equation (7) a resonant contribution, described by means of a Gaussian parametrization formula

$$f(W) = \frac{1}{\sigma\sqrt{2\pi}} e^{-\frac{1}{2}\left(\frac{W-M}{\sigma}\right)^2} \tag{8}$$

In Equation (8), M and σ are used to parametrize the mass and the width of the resonant state, respectively. This parametrization approach was used due to the constraints of the different datasets used. The scan data of BESIII and the ISR data of Belle have very different errors on the energy bin and the chosen distribution provides a more reliable fit with respect to the expected Breit–Wigner one.

Figure 3 shows the plot of the fit to the BESIII and Belle data. The reduced $\chi^2 = 0.34$ indicates that the addition of the resonance is preferred for the fitting of both sam-

ples. The fit results are the following: $M_Y = (4639 \pm 7)\,\mathrm{MeV}/c^2$, $\Gamma_Y = (17 \pm 5)\,\mathrm{MeV}$, $\Lambda_0 = (0.167 \pm 20)\,\mathrm{MeV}$, $\sigma_{\mathrm{thr.}}^{\Lambda_c} = (221 \pm 10)\,\mathrm{pb}$, where all the errors are symmetrical and can be interpreted as 1σ deviations. These values can be compared with the PDG [31] values: $M_{\psi(4660)} = (4630 \pm 6)\,\mathrm{MeV}/c^2$, $\Gamma_{\psi(4660)} = (62^{+9}_{-7})\,\mathrm{MeV}$. Although the mass is in good agreement, the present model finds a smaller width for the $\psi(4660)$. The smaller width shows that this choice of parametrization has some limits. On the one hand, since the points above the resonance peak are described by the non-resonant component, the width becomes smaller with respect to the value measured in [6]. On the other hand, a more natural Breit–Wigner parametrization, that takes into account the vicinity of the threshold, was tested, but with the present data the fits did not converge. Moreover, since the main goal of this work was to extract the threshold behavior rather than the $\psi(4660)$ parameters, we support the Gaussian description that provides a reasonable agreement with the data and provides a ball-park prediction for future measurements of the cross sections in this energy region.

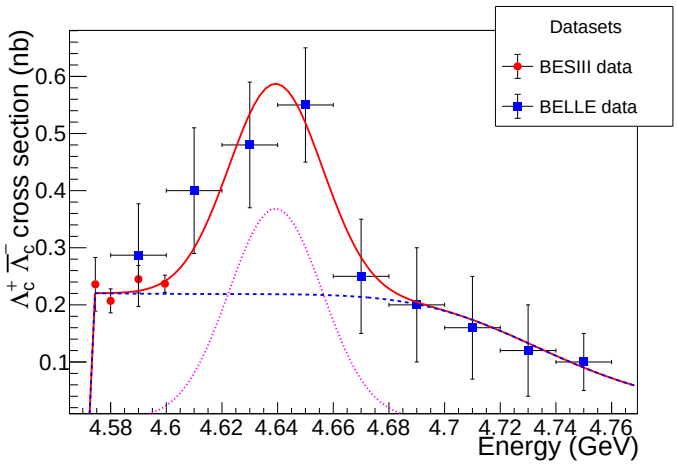

Figure 3. Fit to BESIII [11] and Belle data [6] close to the $\Lambda_c^+\bar{\Lambda}_c^-$ threshold with both resonant and non-resonant contributions. The red dots with error bars indicate the BESIII experimental data, the blue squares indicate the Belle data. The red line indicates the sum of the two contributions. The dashed blue line represents the non-resonant contribution of the fit, whereas the dotted magenta line represents the Breit–Wigner component. Both curves have arbitrary normalization. The first Belle data in [6] are not presented in the plot, as discussed in the introduction.

Table 1 shows this prediction, in the case of resonant and non-resonant trend behavior, as already mentioned in the previous paragraph. The difference between the results is quite significant to allow the experiments to firmly address whether a resonance exists.

4. Summary

The cross section $\sigma(e^+e^- \to \Lambda_c^+\bar{\Lambda}_c^-)$ seems to display two different trends in BESIII and BELLE results. In this work, we proposed a phenomenological description of this cross section based on a strong version of the Coulomb correction, that, being particularly effective at low velocity, could be responsible for the sharp rise experimentally observed at the $\Lambda_c^+\bar{\Lambda}_c^-$ production threshold.

This kind of correction was successfully tested in the case of protons, i.e., for the $\sigma(e^+e^- \to p\bar{p})$ cross section, which has been well measured by several experiments, and then applied to the BESIII and Belle $\Lambda_c^+\bar{\Lambda}_c^-$ data. By adding a resonant contribution, it is also possible to cover the resonant behavior shown in the BELLE data. The agreement with the PDG [31] mass was within 1σ, whereas the width was found to be smaller due to the addition of the continuum. The quality of the fits showed that both the resonant and non-resonant models are viable options (reduced χ^2 = 0.34 and 2 respectively), owing to the large errors in the BELLE data, but with a preference for the former. In the future, BESIII [32] and Belle II will collect more data to deepen the understanding in the studied energy region

and the cross section of charmed baryons. Finally, if the resonant behaviour is confirmed, the same data will be used to provide a more proper description of the $\psi(4660)$ parameters in this final state, possibly taking into account the effect of the threshold vicinity.

Author Contributions: Conceptualization: R.B.F., S.P.; methodology, S.P.; writing—original draft preparation, G.M., S.P., writing—review and editing: A.A., S.B., I.B., M.B., D.B., F.B., A.B., A.C., G.C., F.C., F.D.M., M.D.D.R.R., M.D., R.F., L.F., G.F., L.G., I.G., S.G., M.G., L.L., S.L., M.M., A.M., S.M. (Simonetta Marcello), S.M. (Sara Morgante), E.P., P.P., A.R., M.S., S.S. (Stefano Sosio) and S.S. (Stefano Spataro); funding acquisition: M.M., G.C., M.G., M.B., S.P. All authors have read and agreed to the published version of the manuscript.

Funding: This research was funded by the project FEST of the call RISE-MSCA-H2020-2019 and by the STRONG-2020 European Union's Horizon 2020 research and innovation programme under grant agreement No 824093. Two of the authors (Ilaria Balossino and Giulio Mezzadri) are also supported by the CAS President's International Fellowship Initiative Postdoctoral Researchers funding.

Acknowledgments: We would like to thank Weiping Wang and Huang Guangshun for profitable discussions in the preparation of this article. This work is partially supported by the project FEST of the call RISE-MSCA-H2020-2019 and by the STRONG-2020 European Union's Horizon 2020 research and innovation programme under grant agreement No 824093. Two of the authors (Ilaria Balossino and Giulio Mezzadri) are also supported by the CAS President's International Fellowship Initiative Postdoctoral Researchers funding.

Conflicts of Interest: The authors declare no conflict of interest. The funders had no role in the design of the study; in the collection, analyses, or interpretation of data; in the writing of the manuscript, or in the decision to publish the results.

References

1. Ablikim, M. et al. [BESIII Collaboration]. Measurement of proton electromagnetic form factors in the time-link region using initial stare radiation at BESIII. *Phys. Lett. B* **2021**, *817*, 136328. [CrossRef]
2. Ablikim, M. et al. [BESIII Collaboration]. New Features the Electromagnetic Structure of the Neutron. *arXiv* **2021**, arXiv:2103.12486.
3. Ablikim, M. et al. [BESIII Collaboration]. Observation of a cross-section enhancement near mass threshold in $e^+e^- \to \Lambda\bar{\Lambda}$. *Phys. Rev. D* **2018**, *97*, 032013. [CrossRef]
4. Ablikim, M. et al. [BESIII Collaboration]. Measurement of Σ^+ and Σ^- time-like electromagnetic form factors for center-of-mass energies from 2.3864 to 3.0200 GeV. *Phys. Lett. B* **2021**, *814*, 136110. [CrossRef]
5. Ablikim, M. et al. [BESIII Collaboration]. Measurement of cross section for $e^+e^- \to \Xi^-\bar{\Xi}^+$ near threshold at BESIII. *Phys. Rev. D* **2021**, *103*, 012005. [CrossRef]
6. Pakhlova, G. et al. [Belle Collaboration]. Observation of a near-threshold enhancement in the $e^+e^- \to \Lambda_c^+\bar{\Lambda}_c^-$ cross section using initial-state radiation. *Phys. Rev. Lett.* **2008**, *101*, 172001. [CrossRef] [PubMed]
7. Wang, X.L. et al. [BELLE Collaboration]. Measurement of $e^+e^- \to \pi^+\pi^-\psi(2S)$ via Initial State Radiation at Belle. *Phys. Rev. D* **2015**, *91*, 112007. [CrossRef]
8. Lees, J.P. et al. [BaBar Collaboration]. Study of the reaction $e^+e^- \to \psi(2S)\pi^+\pi^-$ via initial-state radiation at BaBar. *Phys. Rev. D* **2014**, *89*, 111103. [CrossRef]
9. Godfrey, S.; Isgur, N. Mesons in a Relativized Quark Model with Chromodynamics *Phys. Rev. D* **1985**, *32*, 189–231. [CrossRef]
10. Brambilla, N.; Eidelman, S.; Hanhart, C.; Nefediev, A.; Shen, C.-P.; Thomas, C.E.; Vairo, A.; Yuan, C.-Z. The XYZ states: Experimental and theoretical status and perspective. *Phys. Rep.* **2020**, *873*, 1–154. [CrossRef]
11. Ablikim, M. et al. [BESIII Collaboration]. *Precision measurement of* $e^+e^- \to \Lambda_c^+\bar{\Lambda}_c^-$ *cross section near threshold*. *Phys. Rev. Lett.* **2018**, *120*, 132001.
12. Dai, L.-Y.; Haidenbauer, J.; Meissner, U.-G. Re-examining the $X(4360)$ resonance in the reaction $e^+e^- \to \Lambda_c^+\bar{\Lambda}_c^-$. *Phys. Rev. D* **2017**, *96*, 116001. [CrossRef]
13. Epelbaum, E.; Hammer, H.-W.; Meissner, U.-G. Modern Theory of Nuclear Forces. *Rev. Mod. Phys.* **2009**, *81*, 1773–1825. [CrossRef]
14. Epelbaum, E.; Krebs, H.; Meissner, U.-G. Improved chiral nucleon-nucleon potential up to next-to-next-to-next-to-leading order. *Eur. Phys. J. A* **2015**, *51*, 53. [CrossRef]
15. Landau, L.; Lifschitz, E. *Course of Theoretical Physics*, 2nd ed.; Pergamon Press: London, UK, 1982; Volume 4.
16. Sakharov, A.D. Interaction of Electron and Positron in Pair Production. *Zh. Eksp. Teor. Fiz* **1948**, *18*, 631–635.
17. Ablikim, M. et al. [BESIII Collaboration]. Measurement of proton electromagnetic form factors in $e^+e^- \to p\bar{p}$ in the energy region 2.00 - 3.08 GeV. *Phys. Rev. Lett.* **2020**, *124*, 042001. [CrossRef]
18. Ablikim, M. et al. [BESIII Collaboration]. Study of the process $e^+e^- \to p\bar{p}$ via initial state radiation at BESIII. *Phys. Rev. D* **2019**, *99*, 092002. [CrossRef]

19. Solodov, E.P. et al. [CMD-3 Collaboration]. The $N\bar{N}$ and multihadron production at the threshold at VEPP2000. *EPJ Web Conf.* **2019**, *212*, 07002. [CrossRef]
20. Aubert, B. et al. [BaBar Collaboration]. A Study of $e^+e^- \to p\bar{p}$ using initial state radiation with BABAR. *Phys. Rev. D* **2006**, *73*, 012005. [CrossRef]
21. Lees, J.P. et al. [BaBar Collaboration]. Study of $e^+e^- \to p\bar{p}$ via initial-state radiation at BABAR. *Phys. Rev. D* **2013**, *87*, 092005.
22. Baldini, R.; Pacetti, S.; Zallo, A.; Zichichi, A. Unexpected features of $e^+e^- \to p\bar{p}$ and $e^+e^- \to \Lambda\bar{\Lambda}$ cross section near threshold. *Eur. Phys. J. A* **2009**, *39*, 315–321. [CrossRef]
23. Baldini, R.; Pacetti, S.; Zallo, A. No Sommerfeld resummation factor in $e^+e^- \to p\bar{p}$? *Eur. Phys. J A* **2012**, *48*, 33. [CrossRef]
24. Kerbikov, B.; Stavinsky, A.; Fedotov, V. Model independent view on the low mass proton anti-proton enhancement. *Phys. Rev. C* **2004**, *69*, 055205. [CrossRef]
25. Bugg, D.V. Reintepreting several narrow resonances as threshold cusps. *Phys. Lett. B* **2004**, *598*, 8. [CrossRef]
26. Zou, B.S.; Chiang, H.C. One pion exchange final state interaction and the p anti-p near threshold enhancement in $J/\psi \to \gamma p\bar{p}$ decays. *Phys. Rev. D* **2004**, *69*, 034004. [CrossRef]
27. Loiseau, B.; Wycech, S. Antiproton-proton channels in J/psi decays. *Phys. Rev. C* **2005**, *72*, 011001. [CrossRef]
28. Haidenbauer, J.; Meissner, U.-G.; Sibirtsev, A. Near Threshold p anti-p enhancement in B and J/psi decay. *Phys. Rev. D* **2006**, *74*, 017501. [CrossRef]
29. Sibirtsev , A.; Haidenbauer, J.; Krewald, S.; Meissner, U.-G.; Thomas, A.W. Near threshold enhancement of the p anti-p mass spectrum in J/psi decay. *Phys. Rev. D* **2005**, *71*, 054010. [CrossRef]
30. Dmitriev, V.F.; Milstein, A.I. Final state interaction effects in the $e^+e^- \to N\bar{N}$ process near threshold. *Phys. Lett. B* **2007**, *658*, 13. [CrossRef]
31. Zyla, P.A. et al. [Particle Data Group]. The Review of Particle Physics (2021) *Prog. Theor. Exp. Phys.* **2020**, *2020*, 083C01. [CrossRef]
32. Ablikim, M. et al. [BESIII Collaboration]. Future Physics Programme of BESIII. *Chin. Phys. C* **2020** 44, 040001.